

# The nonequilibrium evolution near the phase boundary

Xiaobing Li,<sup>1</sup> Yuming Zhong,<sup>1</sup> Ranran Guo,<sup>1</sup> Mingmei Xu,<sup>1,\*</sup> Jinghua Fu,<sup>1</sup> and Yuanfang Wu<sup>1,†</sup>

<sup>1</sup>Key Laboratory of Quark and Lepton Physics (MOE) and Institute of Particle Physics,  
Central China Normal University, Wuhan 430079, China

(Dated: May 31, 2023)

We study the nonequilibrium evolution near the phase boundary of the 3D Ising model, and find that the average of relaxation time (RT) near the first-order phase transition line (1st-PTL) is significantly larger than that near the critical point (CP). As the system size increases, the average of RT near the 1st-PTL increases at a higher power compared to that near the CP. We further show that RT near the 1st-PTL is not only non-self-averaging, but actually self-diverging: relative variance of RT increases with system size. The presence of coexisting and metastable states results in a substantial increase in randomness near the 1st-PTL, making it difficult to achieve equilibrium.

One important class of phase boundaries consists of the first-order phase transition line (1st-PTL), the critical point (CP), and the crossover region. This type of phase boundary is common to a variety of systems, including the liquid-gas transition [1], magnetic transition [2], metal-insulator transition [3], quark deconfinement, and chiral phase transition in quantum chromodynamics (QCD) [4], among others. The characteristics and properties of the matter state undergo significant changes at or near the phase boundary, making it a subject of great interest.

The static properties of the CP have been extensively studied and are well-known [5–7]. For instance, in the thermodynamic limit, the correlation length  $\xi$  diverges at the critical temperature  $T_c$ , and the static critical exponents typically take fractional values. In the vicinity of  $T_c$ , the autocorrelation time increases with the correlation length, a phenomenon known as critical slowing down [5]. This increase follows a power-law with respect to the correlation length  $\xi$  or the characteristic length of the lattice size  $L$ , governed by the dynamic critical exponent  $z$ . The exponent describes the nonequilibrium dynamics [8, 9]. Furthermore, as the system size increases, the relative variance of magnetization or susceptibility approaches a constant value, indicating non-self-averaging behavior at the CP [10–13].

At the 1st-PTL, the correlation length still diverges, but the static exponents are typically integers [14–16] which is in contrast to the fractional values observed at the CP. However, the dynamic properties at the 1st-PTL have not been fully explored yet. Initially, exponential slowing down was observed [17, 18] and referred to as *supercritical slowing down*, which resulted from deterioration in the simulation algorithm. By introducing the multicanonical algorithm, this type of slowing down was improved to follow a power-law. Subsequently, slowing down near the boundary of the coexisting region was observed in solutions of the dynamical mean-field theory of Mott-Hubbard transition [19] and later in mechanically

induced adsorption-stretching transitions [20]. Non-self-averaging behavior at the 1st-PTL has been observed only in the isotropic-to-nematic transition in liquid crystals [21].

To verify the dynamic properties in different regions of the phase boundary, it is necessary to study the nonequilibrium evolution near the entire phase boundary. The dynamical evolution is commonly described by the Langevin equation [1] and various relaxation models, such as the kinetic Ising model [22] or models A, B, C, etc., classified by the renormalization group [8]. Initially, the dynamical solutions were limited to the crossover region [23], but later they were extended to include the 1st-PTL region [24].

Recently, individual relaxation processes near the CP in the 3D Ising model have been simulated using the Metropolis algorithm [25]. The relaxation time (RT) is defined as the number of sweeps required for the order parameter to reach its equilibrium value. It has been observed that the order parameter approaches its equilibrium value exponentially, which aligns with the behavior predicted by the Langevin equation [1] and a mean-field approximation of relaxation in Ising model [26]. To characterize the relaxation of a sample, the average of RT is introduced. It has been demonstrated that at the critical temperature, the average of RT follows a power-law increase with system size, and the dynamic exponent is consistent with the dynamic universality class of model A [8, 27].

In this letter, we employ this method to investigate the nonequilibrium evolution near the phase boundary of the 3D Ising model. We begin by considering random initial configurations and present the average of RT on the phase plane for a specific system size of  $L=60$ . Subsequently, we discuss the self-averaging properties of RT at the phase boundary. Furthermore, we provide and analyze the results obtained from starting the simulations with a high-temperature state and a polarized initial state at the boundary. Finally, we conclude with a brief summary of our findings.

The CP of the 3D Ising model belongs to the  $Z(2)$  symmetry group. Various physical systems exhibit the same universality class as the 3D Ising model. Exam-

\*Electronic address: xumm@cnu.edu.cn

†Electronic address: wuyf@cnu.edu.cn

ples include the liquid-gas transition, magnetic transition, quark deconfinement, and chiral phase transition in QCD [28]. The 3D Ising model considers a three-dimensional simple cubic lattice composed of  $N = L^3$  sites, where  $L$  is called the system size. Every site  $i$  is occupied by a spin,  $s_i$ . The spin can be in one of two states, either spin-up,  $s_i = +1$ , or spin-down,  $s_i = -1$ . The total energy of a system of  $N$  spins with a constant nearest-neighbor interaction  $J$  placed in a uniform external field  $H$  is

$$E_{\{s_i\}} = -J \sum_{\langle ij \rangle} s_i s_j - H \sum_{i=1}^N s_i, \quad (1)$$

where the notation  $\langle ij \rangle$  restricts the sum to run over all the nearest neighbor spins. The per-spin magnetization is

$$m = \frac{1}{N} \sum_{i=1}^N s_i. \quad (2)$$

When the external field  $H$  takes zero, there is an ordered phase at low temperature where  $|m|$  is close to unity. At high temperature, there is a disordered phase where  $|m|$  is close to zero. A phase transition from a high-temperature disordered phase to a low-temperature ordered phase is anticipated which is continuous and called the Curie point, i.e. the critical point. Below the critical temperature  $T_c$ , as  $H$  changes sign, two phases with opposite directions of magnetization undergo a 1st-PT. The phase boundary of the model consists of the 1st-PTL at  $H = 0$  with  $T < 4.51$  and the CP at  $T_c = 4.51$  [29].

Metropolis algorithm [30], as a local dynamics of Glauber type [22], is suitable for studying nonequilibrium evolution [31, 32]. Starting from an initial configuration, Metropolis algorithm flips one single spin at each step during the evolution. Whether a spin flips depends on the acceptance probability  $A(\mathbf{u} \rightarrow \mathbf{v})$ , which is given by

$$A(\mathbf{u} \rightarrow \mathbf{v}) = \begin{cases} e^{-(E_{\mathbf{v}} - E_{\mathbf{u}})/k_B T} & \text{if } E_{\mathbf{v}} - E_{\mathbf{u}} > 0, \\ 1 & \text{otherwise.} \end{cases} \quad (3)$$

$\mathbf{u}$  and  $\mathbf{v}$  represent the state of the system before and after flipping this spin. If  $A(\mathbf{u} \rightarrow \mathbf{v}) = 1$ , the spin is flipped. If  $A(\mathbf{u} \rightarrow \mathbf{v}) < 1$ , a random number  $r$  ( $0 < r < 1$ ) is generated. If  $A(\mathbf{u} \rightarrow \mathbf{v}) > r$ , the spin is flipped, otherwise, the spin keeps its original state. The testing of one single spin is called a Monte Carlo step. When  $N$  Monte Carlo steps are completed, every spin in the lattice has been tested for flipping and *one sweep* is completed. In this way, the configuration of the system is updated once a sweep. After evolving enough sweeps, the magnetization approaches a steady value and the system reaches equilibrium. Relaxation time of a process is defined by the number of sweeps required for magnetization to reach a stable value [25].

To quantify the RT of a sample, the average of RT is

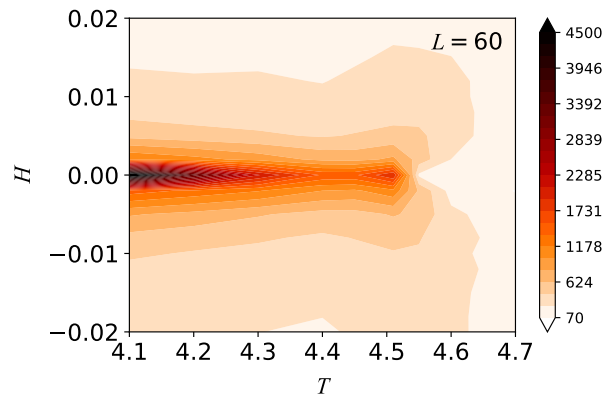


FIG. 1: A contour plot of the average of RT  $\bar{\tau}$  on the phase plane of the 3D Ising model for a system size  $L = 60$ .

suggested as [25],

$$\bar{\tau} = \frac{1}{n} \sum_{i=1}^n \tau^i, \quad (4)$$

where  $n$  is the total number of evolution processes,  $\tau^i$  is RT of the  $i^{\text{th}}$  process.

Figure 1 presents a contour plot of the average of RT on the  $T$ - $H$  phase plane for a fixed system size of  $L = 60$ , starting from random initial configurations. The color scheme ranges from white to red to black, representing the average of RT values that span from less than a hundred to over four thousand. The phase boundary is depicted by the line  $H = 0$ .

Figure 1 illustrates that in regions far from the phase boundary, the color appears light, indicating a small average of RT. However, a dark-red point emerges around  $T_c = 4.51$ , indicating a large average of RT, which is consistent with the phenomenon of critical slowing down as expected.

Along the 1st-PTL, the color becomes progressively darker as the temperature decreases, eventually turning completely black when the temperature drops below 4.2. Simultaneously, on the low-temperature side, specifically in the direction of the external field, the color transitions rapidly to black near  $H = 0$ . These observations indicate that the relaxation process near the 1st-PTL is considerably slower compared to that near the CP, and can be characterized as *ultra-slowing down*.

Ultra-slowing down indicates a higher level of uncertainty and randomness. This can be attributed to the more complex structure of the free energy at the 1st-PT compared to the CP. The 1st-PT represents a transition between distinct internal states, where both upward and downward magnetized phases coexist along the transition line. In the equilibrium state, the system can be either in an upward or downward magnetized state with equal probability, effectively doubling the number of possible states. Near the 1st-PTL, some of these possible states manifest as metastable states, as indicated

by the spinodal curve [19]. The presence of coexisting and metastable states significantly increases the instability, uncertainty, and randomness in the equilibrium state. This heightened randomness results in a much longer RT. Consequently, achieving equilibrium at the 1st-PT is a challenging task.

To show the system size dependence of a nonequilibrium evolution, Fig. 2(a) presents a double-logarithmic plot illustrating the variation of the average of RT  $\bar{\tau}$  with system size  $L$  for three different temperatures at the boundary  $H = 0$ . The data points corresponding to  $T_c = 4.51$  are denoted by red squares, while the data points below  $T_c$  are represented by blue circles and purple triangles. The error bars indicate only the statistical errors.

Both at the CP and the 1st-PTL, the average of RT ( $\bar{\tau}$ ) increases with system size  $L$ , and can be accurately described by a power-law relationship, i.e.,

$$\bar{\tau} \propto L^z. \quad (5)$$

The power exponent  $z$ , which corresponds to the slope of the fitting line, represents the dynamic exponent. The values of the dynamic exponent are provided in the legend of Fig. 2(a). The critical dynamic exponent  $z = 2.005 \pm 0.012$  is obtained by fitting from  $L = 20$  to  $L = 100$ , which has higher statistical accuracy and is more precise than the previously reported value of  $z = 2.06 \pm 0.03$  [25]. Both values are consistent with the dynamic universality class of model A [8, 27]. This shows that the average of RT, as defined by Eq. (4), serves as a similar role to the autocorrelation time. At the 1st-PTL, the dynamic exponent  $z$  is larger than that at the CP. As a result, the average of RT at the 1st-PTL increases more rapidly with system size compared to that at the CP.

To further investigate the change in the randomness of the RT with system size, we examine its self-averaging property. Self-averaging refers to the behavior of the relative variance of an observable  $X$  as the system size increases. It can be defined as follows:

$$R_X = \frac{\overline{X^2} - \bar{X}^2}{\bar{X}^2}, \quad (6)$$

where bar represents the average over the entire sample. If  $R_X$  tends to zero,  $X$  is self-averaging; if  $R_X$  increases,  $X$  is self-diverging. In case of self-averaging, the fluctuation of  $X$  diminishes as the system size increases, and the average of  $X$  converges to the same value. Self-diverging means divergent fluctuations of  $X$  as the system size increases.

At the boundary ( $H = 0$ ), the relative variance of  $\tau$  is plotted against the system size  $L$  for three different temperatures in Fig. 2(d). The trend of  $R_\tau$  with system size  $L$  is observed to be significantly different for each temperature. Notably, at the critical temperature  $T_c = 4.51$ ,  $R_\tau$  remains almost constant as the system size increases. In other words, the variance or width of the RT distribution increases with the system size at the same rate as the

average of RT, indicating non-self-averaging behavior of RT. This observation is consistent with other observables studied in the same context [10].

At temperatures  $T = 4.30$  and  $T = 4.20$ , it is observed that the relative variance  $R_\tau$  increases with the system size  $L$ , indicating self-diverging behavior at the 1st-PTL. This behavior is similar to what is observed in liquid crystals [21]. As the system size increases, the variance of RT increases more rapidly than the average of RT and the distribution of RT become wider and flatter. This phenomenon suggests that randomness is significantly amplified with system size, leading to an abnormally increased variance. Such an extremely broad distribution of RT is a characteristic feature of the relaxation near the 1st-PTL.

To explore the behavior away from the boundary, the average of RT is plotted against the system size  $L$  in a double-logarithmic plot for three small external fields at a specific temperature  $T = 4.2$  in Fig. 3(a). The external fields are  $H = 10^{-5}$  (red circles),  $H = 0.001$  (blue triangles), and  $H = 0.02$  (green squares). Figure 3(a) illustrates that for each external field, as the system size increases, the average of RT also increases and can be fitted by a line, similar to the case shown in Fig. 2(a). Consequently, away from the boundary, the average of RT exhibits a power-law relationship with  $L$ .

The power  $z$  for  $H = 10^{-5}$  as presented at the legend of Fig. 3(a) is nearly the same as that observed at the 1st-PTL shown in Fig. 2(a). However, as one moves away from the 1st-PTL along the direction of the external magnetic field,  $z$  gradually decreases. This reduction can be attributed to the alignment tendency of spins with the external magnetic field. As the external field becomes non-zero, the spins tend to align in the direction of the field, thereby reducing the overall randomness in the system.

Furthermore, similar to the case presented in Fig. 3(a), the relative variance  $R_\tau$  is plotted against the system size  $L$  for three external fields in Fig. 3(b). It is observed that self-diverging behavior is only prominent at  $H = 10^{-5}$ , which is the nearest to the 1st-PTL. For larger external fields, such as  $H = 0.001$  and  $H = 0.02$ ,  $R_\tau$  decreases slowly as  $L$  increases, indicating self-averaging of RT. As the deviation from the 1st-PTL becomes further, the self-diverging behavior of RT becomes less pronounced. Therefore, self-diverging behavior is observed not only precisely at the 1st-PTL but also in its close vicinity, while far from the phase boundary, RT exhibits self-averaging behavior.

As demonstrated in our previous paper [25], the initial configuration has a significant impact on the RT. A random initial configuration represents a completely disordered state, indicating a very high temperature. Nonequilibrium evolution from such a high temperature state to the phase boundary can occur spontaneously. To provide a comprehensive analysis, we also include the results for initial states with a temperature of  $T = 4.6$  and a polarized configuration. The middle and right columns of Fig. 2 depict the double-log plot of the average of RT

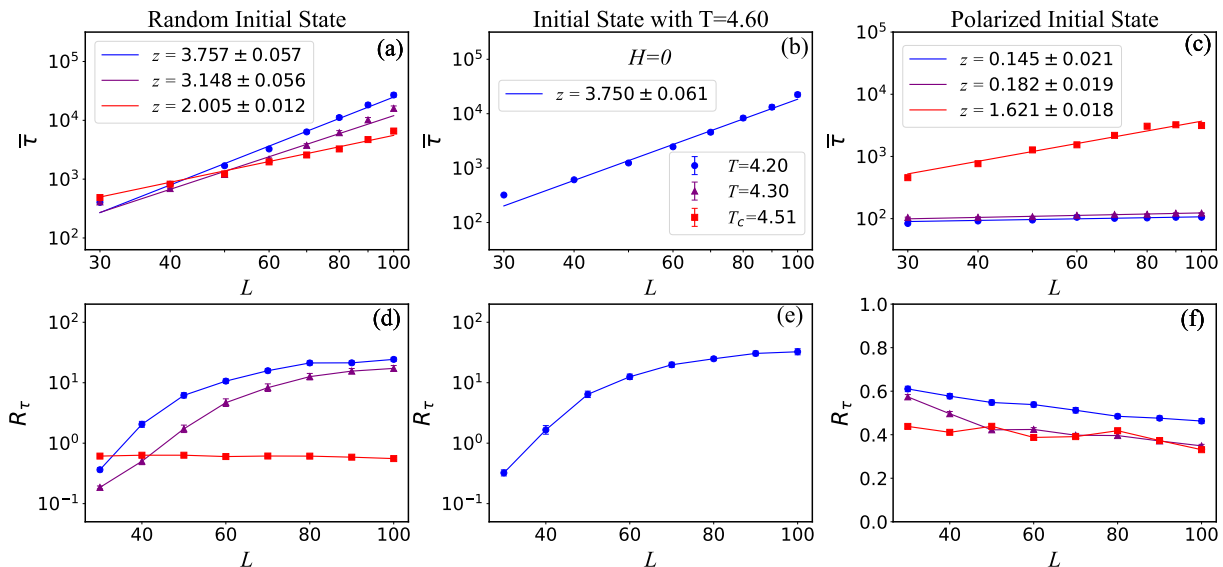


FIG. 2: The finite size scaling of the average of RT for three different initial states: random initial state (a), equilibrium state at  $T = 4.60$  (b), and polarized initial state (c).  $R_\tau$  as a function of  $L$  for each of these cases, denoted as (d), (e), and (f) respectively.

and the relative variance of RT, respectively, as a function of system size.

The initial configuration of Figs. 2(b) and 2(e) corresponds to an equilibrium configuration at  $T = 4.6$ , while the final state temperature is  $T = 4.2$ . Both configurations lie on the boundary  $H = 0$ . It is evident that the initial state with  $T = 4.6$  is less random than, but still very close to, the random initial configuration. The average of RT shown in Fig. 2(b) also exhibits an increase with system size and can be fitted with a straight line, similar to Fig. 2(a), but with a slightly smaller slope  $z$ . Therefore, the divergence of average of RT is not as rapid as in Fig. 2(a) since the reduced randomness has an effect. Simultaneously, the relative variance of RT, as shown in Fig. 2(e), also increases with system size, indicating the occurrence of self-diverging RT.

Figures 2(c) and 2(f) present the average of RT and the relative variance of RT as a function of system size, respectively, starting from a polarized initial configuration for three different temperatures. In Fig. 2(c), it can be observed that the average of RT increases with system size for each temperature and can be fitted with a line. The slope  $z$  at the critical temperature is the largest but smaller than that in Fig. 2(a). The slopes  $z$  for the other two temperatures decrease significantly compared to Fig. 2(a). Additionally, Fig. 2(f) demonstrates that the relative variance of RT decreases with system size for all three temperatures, indicating that RT exhibits self-averaging behavior in this case.

As we are aware, a polarized initial configuration is equivalent to an equilibrium state at a very low temperature. This ordered state possesses a similar structure to the equilibrium states at the 1st-PTL. Consequently, the evolution from a polarized initial configuration to the

states at the 1st-PTL is considerably facile, resulting in a substantial reduction in the average of RT. The self-diverging behavior observed in Fig. 2(d) is completely absent. However, it should be noted that the structure of the polarized configuration still remains distinct from that of the CP. The average of RT towards the CP continues to diverge.

In summary, the Metropolis algorithm has been employed to achieve nonequilibrium evolution from three different types of initial states to the phase boundary of the 3D Ising model.

Firstly, we generate random initial configurations and plot the contour of average of RT on the phase plane for a fixed system size of  $L = 60$ . In comparison to the critical slowing down observed at the critical point,  $\bar{\tau}$  near the 1st-PTL exhibits ultra-slowing down behavior. As the system size increases,  $\bar{\tau}$  near the 1st-PTL follows a power-law increase, similar to the behavior near the CP, but with a larger dynamic exponent.

The self-averaging properties of RT at and near the phase boundary are also examined. As the system size increases, the relative variance of RT near the 1st-PTL increases, eventually converging to a constant value near the CP. Consequently, RT exhibits self-diverging behavior near the 1st-PTL, and non-self-averaging behavior near the CP. The level of randomness near the 1st-PTL is significantly higher compared to the CP. This increased randomness can be attributed to the presence of coexistence and metastable states, which greatly expand the number of possible states and consequently lead to a highly broad distribution of RT. This characteristic of relaxation near the 1st-PTL distinguishes it from the behavior observed at the CP.

The investigation of the external field  $H$  dependence

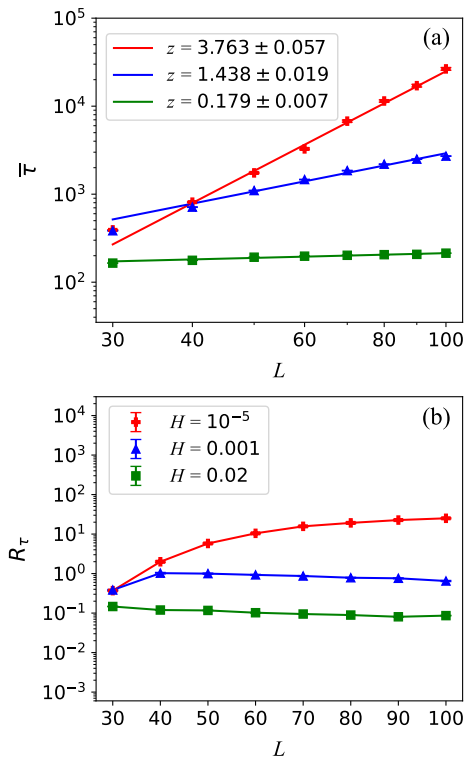


FIG. 3: (a) The finite size scaling of the average of RT for three different values of the external magnetic field at  $T = 4.20$ . (b) The relative variance of RT as a function of system size  $L$  for each of the aforementioned cases.

of the power-law behavior and self-averaging properties of RT provides further confirmation that the violation of self-averaging is directly related to the level of randomness. As  $H$  decreases, the degree of randomness increases, leading to an increase in the dynamic exponent and a transition of RT behavior from self-averaging to non-self-averaging. The proximity to the 1st-PTL intensifies these effects, resulting in a larger dynamic exponent and a more severe violation of self-averaging, ultimately leading to self-diverging behavior.

While the specific value of the dynamic exponent can vary with the model and algorithm employed [34], the characteristics of nonequilibrium relaxation, such as ultra-slowing down and self-diverging at the 1st-PTL, critical slowing down and non-self-averaging, and power-law behavior with increasing system size, are expected to be independent of the specific model and algorithm used. These qualitative features of nonequilibrium relaxation are general phenomena that can be observed across different models and algorithms, providing insights into the universal behavior of systems near phase transitions.

#### Acknowledgement

This research was funded by the National Key Research and Development Program of China, grant number 2022YFA1604900, and the National Natural Science Foundation of China, grant number 12275102. The numerical simulations have been performed on the GPU cluster in the Nuclear Science Computing Center at Central China Normal University (NSC3). We are grateful to Mr. Yu Zhou for assisting us in describing the results.

- 
- [1] L. D. Landau and E. M. Lifshitz, *Statistical Physics Part 1*, 3rd ed. (Pergamon Press, Oxford, 1980).
- [2] D. E. Laughlin, *Metallurgical and Materials Transactions A* 50, 2555 (2019).
- [3] N. Tong, S. Shen and F. Pu, *Phys. Rev. B* 64, 235109 (2001).
- [4] A. Bzdak, S. Esumi, V. Koch, J. Liao, M. Stephanov, N. Xu, *Phys. Rep.* 853, 1 (2020).
- [5] M. E. J. Newman and G. T. Barkema, *Monte Carlo Methods in Statistical Physics* (Oxford University Press, Oxford, 1999).
- [6] V. Privman, *Finite Size Scaling and Numerical Simulation of Statistical Systems* (World Scientific, Singapore, 1990).
- [7] J. Cardy, *Scaling and Renormalization in Statistical Physics* (Cambridge University Press, 1996).
- [8] P.C. Hohenberg and B.I. Halperin, *Rev. Mod. Phys.* 49, 435 (1977).
- [9] M. Hasenbusch, *Phys. Rev. E* 101, 022126 (2020).
- [10] S. Wiseman and E. Domany, *Phys. Rev. E* 52, 3469 (1995).
- [11] A. Malakis and N.G. Fytas, *Phys. Rev. E* 73, 016109 (2006).
- [12] G. Parisi and N. Sourlas, *Phys. Rev. Lett.* 89, 257204 (2002).
- [13] K. A. Pronin, *Physica A* 596, 127180 (2022).
- [14] K. Binder, *Rep. Prog. Phys.* 50, 783 (1987).
- [15] M. E. Fisher, A. N. Berker, *Phys. Rev. B* 26, 2507 (1982).
- [16] Y. Zhang, Y. Zhao, L. Chen, X. Pan, M. Xu, Z. Li, Y. Zhou, Y. Wu, *Phys. Rev. E* 100, 052146 (2019).
- [17] B. Berg and T. Neuhaus, *Phys. Rev. Lett.* 68, 9 (1992).
- [18] B. Berg, arXiv:cond-max/9909236, published as *Fields Institute Communications* 26, 1 (2000).
- [19] J. Joo and V. Oudovenko, *Phys. Rev. B* 64, 193102 (2001).
- [20] S. Zhang, S. Qi, L. I. Klushin, A. M. Skvortsov, D. Yan, and F. Schmid, *J. Chem. Phys.* 147, 064902 (2017).
- [21] J.M. Fish, R.L.C. Vink, *Phys. Rev. Lett.* 105, 147801 (2010).
- [22] N. Menyhard and G. Odor, *Brazilian Journal of Physics* 30, 113 (2000).
- [23] S. Mukherjee, R. Venugopalan, and Y. Yin, *Phys. Rev. C* 92, 034912 (2015).
- [24] Lijia Jiang, Jingyi Chao, *Eur. Phys. J. A* 59, 30 (2023).
- [25] Xiaobing Li, Mingmei Xu, Yanhua Zhang, Zhiming Li, Yu Zhou, Jinghua Fu and Yuanfang Wu, *Phys. Rev. C* 105, 064904 (2022).
- [26] I. Tikader and M. Acharyya, arXiv:2305.10765.
- [27] J.V. Roth, L. von Smekal, arXiv:2303.11817.

- [28] M. A. Stephanov, K. Rajagopal and E. Shuryak, Phys. Rev. Lett. 81, 4816 (1998).
- [29] A. L. Talapov and H. W. Blote, J. Phys. A: Math. Gen. 29, 5727 (1996).
- [30] N. Metropolis, A. W. Rosenbluth, M. N. Rosenbluth, A. H. Teller and E. Teller, J. Chem. Phys. 21, 1087 (1953).
- [31] C.-W. Liu, A. Polkovnikov and A. W. Sandvik, Phys. Rev. B 89, 054307 (2014).
- [32] M. Acharyya, Phys. Rev. E 56, 2407 (1997).
- [33] Y. Aoki, G. Endrodi, Z. Fodor, S. D. Katz and K. K. Szabo, Nature 443, 675 (2006).
- [34] T. Fischer et al., J. Phys.: Condens. Matter 22, 104123 (2010).